SCIENTIFIC REPORTS

OPEN

SUBJECT AREAS:
SELF-ASSEMBLY
BIOPOLYMERS
NANOSCALE BIOPHYSICS
ORGANIZING MATERIALS WITH DNA

Received
12 June 2013

Accepted
16 December 2013

Published
13 January 2014

Correspondence and requests for materials should be addressed to K.Y. (keyoshik@mail.doshisha.ac.jp)

# Self-organized patterning through the dynamic segregation of DNA and silica nanoparticles

Rastko Joksimovic[1,2], Shun Watanabe[3], Sven Riemer[1], Michael Gradzielski[1] & Kenichi Yoshikawa[3]

[1]Technische Universität Berlin, Institut für Chemie, Strasse des 17. Juni 124, Sekr. TC7, D-10623 Berlin, Germany, [2]WPI-AIMR, Tohoku University, 2-1-1 Katahira, Aoba-ku, Sendai 980-8577, Japan, [3]Faculty of Life and Medical Sciences, Doshisha University, Miyakodani, Kyotanabe, Kyoto 610-0394, Japan.

**Exotic pattern formation as a result of drying of an aqueous solution containing DNA and silica nanoparticles is reported. The pattern due to segregation was found to critically depend on the relative ratio of nanoparticles and DNA, as revealed by polarization microscopy, scanning electron microscopy, and fluorescence microscopy. The blurred radial pattern that is usually observed in the drying of a colloidal solution was shown to be vividly sharpened in the presence of DNA. Uniquely curved, crescent-shaped micrometer-scale domains are generated in regions that are rich in nanoparticles. The characteristic segregated patterns observed in the present study are interpreted in terms of a large aspect ratio between the persistence length (~50 nm) and the diameter (~2 nm) of double-stranded DNA, and the relatively small silica nanoparticles (radius: 5 nm).**

Drying droplets have attracted considerable interest from the scientific community, especially since Deggan[1,2] reported coffee ring deposits resulting from the evaporation of a sessile nanofluid drop on a hydrophilic surface. This phenomenon is the result of the cooperation between pinning of the contact line and differential evaporation over the surface[3,4].

Many of these studies have focused on drying droplets containing nanoparticles[5–9]. An interesting phenomenon that has been characterized is the formation of cracks during the drying of silica nanoparticle suspensions[10–12]. Drying droplets can fracture to generate regular patterns, thereby forming structured films. Due to water evaporation, the accumulation of particles and ionic species near the surface leads to the formation of a gel that subsequently shrinks within a confined geometry, which results in high levels of stress and the formation of cracks. As a result, linear cracks that are arranged in parallel and measure up to several hundreds of micrometers are sometimes generated[13,14].

The drying of DNA suspension has been intensely studied, with DNA being a well-defined very stiff colloidal object[15–19]. Around 15 years ago, Fang and Remeker[20] studied the production of DNA fibers by electrospinning from aqueous solutions of DNA. Jing et al[21]. observed the elongation and fixation of DNA molecules on derivatized surfaces by means of a fluid flow arising within evaporating droplets. In the same year 1998, Wang et al[15]. reported the imaging of elongated DNA molecules after droplet drying by scanning force microscopy. Through the use of single-molecule observation with fluorescence microscopy, Abramchuk et al[22]. observed characteristic conformational changes in individual giant DNA (T4 DNA, 165 kbp, corresponding to a total length of ~50 μm) molecules in the vicinity of the contact line of a drying droplet. A high level of stretching was observed at the droplet periphery and a random coil state was observed in the central region. Smalyukh et al[23]. observed the formation of ringlike deposits in drying droplets of DNA (48.5 kbp). At the droplet edge, DNA molecules form a lyotropic crystal with a concentric chain. In the final phase, the contact line retracts and radial stress causes undulations at the rim with the formation of a periodic pattern. Fang et al[19]. studied the evaporation kinetics of droplets containing DNA and measured the distribution of DNA inside the droplets with confocal microscopy. DNA was found to be condensed mostly on the surface of the droplets. Maheschwari et al[24]. observed multi-ring stains due to a pinning-depinning cycle generating new contact lines.

A very interesting topic are the interactions between DNA and nanoparticles, due to the general importance of DNA but also as it is a rather stiff charged colloidal object. It has been reported that negatively charged silica nanoparticles 100 nm in diameter enhance the ability of cationic surfactants to induce genomic T4 DNA compaction[25]. The effect of the particle size (15–100 nm) has also been studied[26], and the results showed that

the effect is more pronounced with smaller nanoparticles. Zhang et al[27]. were the first to report on the drying of droplets containing both large DNA molecules (115 kbp) and silica particles (size ranging from 50 nm to 2.89 μm). They found that high DNA concentrations and low colloidal concentrations favor the formation of the multiple-ring pattern, which had been reported previously by them for DNA only[24], with the difference here that the size of the particles had a significant effect on the drying pattern.

Also, depletion effects of DNA have attracted much interest. They were reported on the conformational properties of T4 DNA in a salt solution of the strongly charged protein bovine serum albumin (BSA)[28,29]. DNA compaction was due to a crowding effect and strong electrostatic repulsion between DNA and BSA, both of which are negatively charged. We also observed[30] the appearance of a partially segregated state in a microsphere due to the interaction between actin filaments and T4 DNA molecules. A similar result was observed in a microsphere with DNA and alginate, a negatively charged polyelectrolyte[31]. We also reported segregation with smaller DNA strands (peak at 500 bp)[32] and PEG. Regarding the segregation of nanoparticles, Gupta et al[33]. reported how PEG-covered 5.2 nm silica nanoparticles dispersed in a poly(methyl methacrylate) matrix segregated to cracks in an adjoining silicon oxide layer.

In our work we were interested in the formation of structured hybrid films, where the ordering is induced by the presence of DNA in a mixed colloidal system, as such structured films are of high relevance for many applications in sensoring, due to their optical properties, controlled wetting properties, etc… We report the emergence of a unique self-organized pattern through the drying of a mixture of DNA (peak at 400 bp, corresponding to a length of around 120 nm) and silica nanoparticles (radius of 5 nm), where these negatively charged species exhibit mutual repulsive interaction in solution and are expected to segregate from each other, thereby forming a kinetically driven pattern. There have been many studies on the interaction of DNA with positively charged species, such as histone and polyamines, but not much attention has been paid to the conformational change of genomic DNA in the presence of negatively charged species. This study is of high importance as the segregation of DNA and negatively charged nanoparticles is a relatively unexplored topic, and a very interesting one as this process is largely controlled by the shape asymmetry of the colloidal components, which should be responsible for the pattern formation. This is a fundamentally important topic to the understanding of pattern formation in colloidally structured films, and it is also of practical interest for manufacturing well-defined films. In particular, the systems studied by us showed an interesting pattern formation that depends on the mixing ratios of DNA and silica nanoparticles employed. The remarkable segregation patterns that resulted from drying were scrutinized by polarization microscopy (PM), high-resolution scanning electron microscopy (HR-SEM), and fluorescence microscopy.

## Results

**Polarization microscopy (PM).** PM was used in order to observe differences between samples with and without DNA, and thereby confirm the influence of DNA on the structure of a dried droplet of colloidal solution in the larger μm-mm size range. The images obtained for a dried drop of a solution containing only nanoparticles (a) and a dried drop of a solution containing both DNA and nanoparticles (b) are shown in Figure 1.

We observed the crack pattern that is usually obtained after the drying of nanoparticle solutions, as reported in the literature[13,14]. The drying wave propagates from the outer rim toward the center of the droplet, and the star-shaped crack pattern is more or less centrally symmetric. DNA clearly influences the cracking process. In particular, a clear crack pattern with pronounced contour enhancement was observed, which is attributable to the specific interaction between DNA and nanoparticles. Interestingly, we observed lateral cracks in addition to radial cracks. These lateral cracks were not observed in the absence of DNA (see Figure 1(a)).

Different NP/dsDNA ratios led to different observations. In particular, for the ratios of 1 : 0.5 and 1 : 0.25, we observe a highly pronounced, star-like pattern, whereas starting from the ratio 1 : 0.167 the pattern is less pronounced and the star-like structure is less clear. The results are presented in the ESI, and this observation will be treated in more detail in the section on the SEM results. Additionally, the crack pattern observed with nanoparticles only was quite fragile. It eventually broke apart, sometimes even during drying. In contrast, such breaking apart was usually not observed for samples with both nanoparticles and DNA for NP/dsDNA ratios higher than 1 : 0.167. Therefore, DNA significantly influences the film's mechanical properties, inducing for instance a reduced brittleness and an increased elasticity.

**Scanning electron microscopy (SEM).** SEM was done in order to gain mesoscopic structural details regarding the formed films. The images for a NP/dsDNA ratio of 1 : 0.5 are shown in Figure 2. This particular ratio gives a remarkable pattern (see especially Figure 2(b)). The observed crescent-shaped domains of micrometer size should be due to segregation between DNA and nanoparticles during drying and are homogeneously distributed throughout the surface.

The NP/dsDNA ratio strongly influenced the drying pattern. Figure 3 shows images for two other lower ratios. As the DNA concentration decreases, the segregation domains have a less homogeneous distribution and are less widespread. Therefore, there is a threshold DNA concentration starting from which the domains show a homogeneous distribution throughout the system. At a ratio

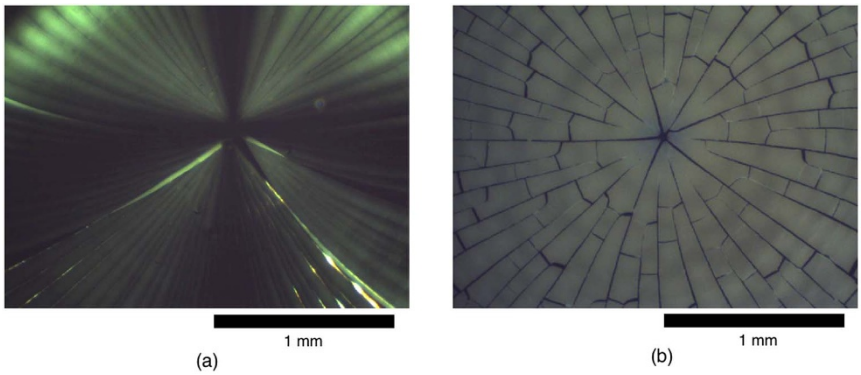


**Figure 1 | PM images obtained after the complete drying of droplets containing (a) nanoparticles only (7.8% wt.) and (b) nanoparticles (NP) at the same concentration with DNA at 20.8 mg · mL$^{-1}$ corresponding to a NP/dsDNA ratio of 1 : 0.5 (2 nanoparticles per double-strand DNA).** The scale bar is 1 mm.

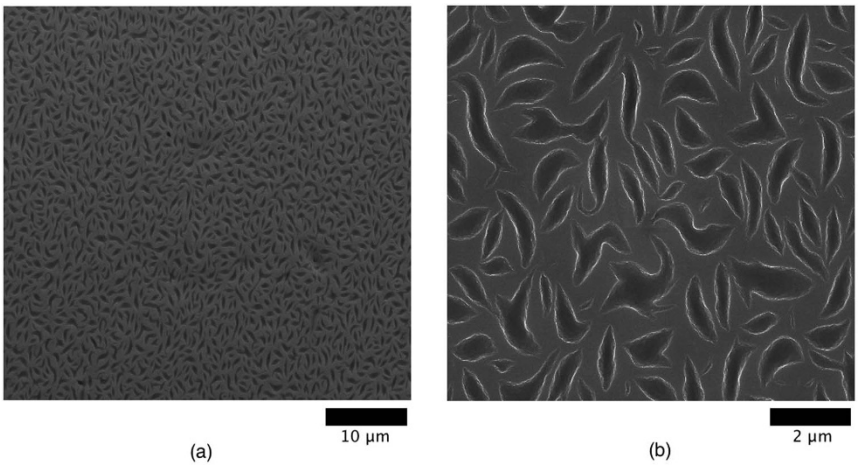


**Figure 2 | HR-SEM images of dried drops for a NP/dsDNA ratio of 1 : 0.5.** The scaling bar corresponds to (a) 10 μm and (b) 2 μm.

of 1 : 0.125 (see ESI), the pattern due to segregation is no longer observed.

**Additional observations.** DNA molecules were stained by the dye YOYO-I and the dried samples were observed by fluorescence microscopy. The result for a NP/dsDNA ratio of 1 : 0.5 is displayed in Figure 4 along with the control (no DNA but at identical dye concentration). It is noted that through such a procedure it becomes possible for us to obtain the optical image with a relatively high magnification. Thus, the scale in Figure 4 corresponds to the SEM image in Figure 2(a). Whereas the fluorescence control sample without DNA exhibits a uniform intensity, the sample with DNA at the ratio 1 : 0.5 shows a point fluorescence pattern which can be correlated to the pattern obtained by SEM (Figure 2(a)). These figures clearly indicate the occurrence of segregation. The comparison with the control sample evidences the domain segregation of DNA, and the comparison with the SEM image confirms that the observed particular domains are due to the presence of DNA. Images obtained at other NP/dsDNA ratios, including with a higher DNA concentration, are available in the ESI. The evolution of the pattern with the DNA concentration has also been evidenced in this case.

TEM is less useful for this study because the samples have to be drastically diluted, which might influence the outcome of drying. However, there was a slight change due to the presence of DNA, since the nanoparticles were more tightly packed after drying without DNA (see ESI).

## Discussion

As mentioned in the introduction, Zhang et al[27]. have reported an experimental observation on drying droplets containing both DNA and silica nanoparticles. They used much longer DNA strands (115 kbp vs. 400 bp), and the silica nanoparticles were also larger (from 50 nm vs. 10 nm in our case). The outcome of the drying process was therefore completely different, especially as short DNA strands behave quite differently from a mechanistic point of view than large DNA strands. The two studies, though being similar in some aspects, are quite distinct with respect to the prevailing colloidal conditions. In our case, we focused on the segregation process between DNA and silica nanoparticles during drying, which was not covered in previous reports.

We have observed a unique segregation pattern between DNA and silica nanoparticles, where both are negatively charged. Recently, it has been shown that, for an aqueous mixture of DNA and albumin, DNA molecules with a size above 100 kbp tend to be repelled from albumin[28,29]. As has been discussed in detail[28,29], an increase in the albumin concentration as a negatively charged globular protein generates the segregation of DNA, because depletion of DNA from highly concentrated albumin results in the increase of free space or entropy due to the fluctuating Brownian motion of the albumin molecules. In other words, the repulsive interaction between DNA and albumin is the essential driving force of the segregation. Thus, we may expect a similar effect for negatively charged nanoparticles, namely to cause the segregation of DNA.

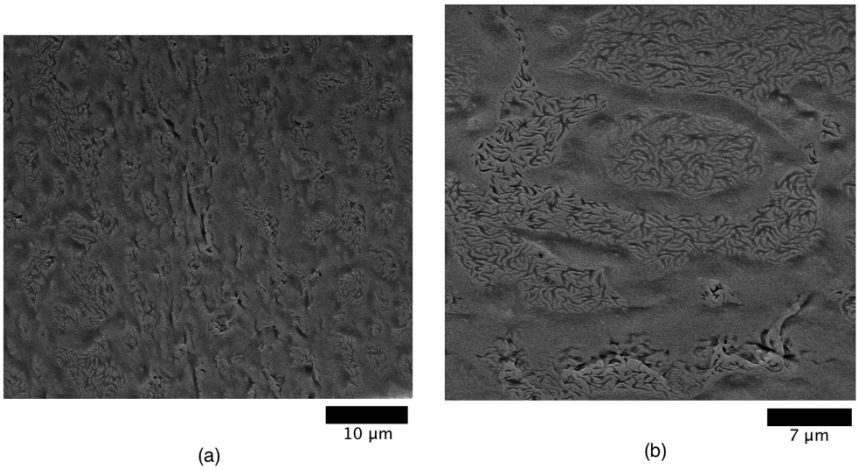


**Figure 3 | HR-SEM images of dried droplets for NP/dsDNA ratios of (a) 1 : 0.25 and (b) 1 : 0.167.** The scaling bar is 10 μm and 7 μm respectively.

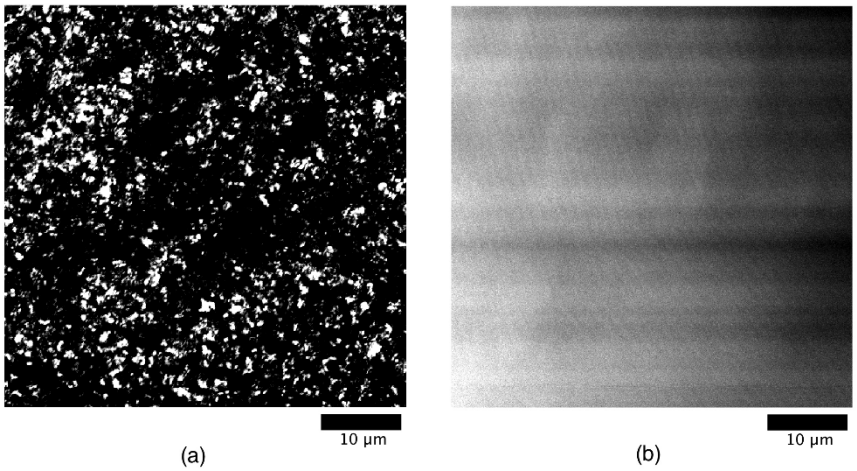


**Figure 4 | Fluorescence microscopic observation.** (a) Image obtained by staining DNA with the dye YOYO-I for the NP/dsDNA ratio 1 : 0.5. (b) Control sample without DNA at the same dye concentration as in (a). The scaling bar is 10 μm.

Our expectation regarding the appearance of an ordered segregation state is supported in particular by the SEM results, especially those for a NP/dsDNA ratio of 1 : 0.5 shown in Figure 2 indicating that DNA and nanoparticles are segregating during the drying process. The homogeneously distributed crescent-shaped domains are apparently due to the presence of DNA since they gradually disappear when the DNA concentration is reduced (see Figure 3). Furthermore, the fluorescence pattern obtained by staining DNA (see Figure 4(a)) corresponds well to the pattern obtained by SEM at a similar magnification, which confirms that the segregation domains observed are due to the presence of DNA.

No segregation was observed in bulk liquid samples, which were isotropic as ascertained by PM. This shows that the present phenomenon only occurs at high enough DNA and nanoparticle concentrations, and in particular under two-dimensional confinement. Also, the influence of the DNA concentration is noteworthy. The pattern observed by PM changes considerably with the DNA concentration (see ESI). This important difference was also noticed by HR-SEM, and one observes two important threshold concentrations. The first concerns the local appearance of segregation domains, and lies somewhere between the ratios of 1 : 0.125 and 1 : 0.167 (see Figure 3(b)). The second concerns the extension of segregation domains throughout the material, and lies somewhere between the ratios of 1 : 0.25 and 1 : 0.5 (see Figure 2). The distribution of the domains becomes homogenous over the entire film, both on the surface and the interior. There should also be an upper limit for domain formation with increasing DNA content, however the concentrations used in this experiment were not high enough for this upper-limit to be observed.

The traditional crack pattern obtained after the drying of colloidal solutions was also observed in this case. Additionally, we noted that the presence of DNA led to more pronounced cracks, and to additional lateral cracks, which were not seen in the sample that contained only nanoparticles. This can be explained by the fact that DNA molecules near a radial crack tend to be expelled to a linear array along the crack, which makes it appear with a higher contrast. We then argue a possible scenario for the appearance of lateral cracks. Due to segregation, some regions have a higher concentration of nanoparticles, which produces an increase in stress away from the radial cracks, which in turns leads to the appearance of additional cracks. Also, the observed segregation domains containing DNA represent regions of lower density. Therefore, the system can break more easily, just as it is easier to break a board that contains holes. It should be noted that the formation of a segregation pattern precedes the appearance of cracks, as with both the radial and lateral cracks on Figure 5. Indeed, the homogeneous distribution is not affected in the vicinity of the cracks. Some domains are even torn apart by the propagating cracks.

The occurrence of phase segregation in the mixture of nanoparticles and DNA implies that there is a discrete transition between the isotropic and ordered phases and can be interpreted in terms of spinodal decomposition[34,35]. Indeed, this is a system of two components that separate into distinct regions with different structural properties leading to a finely dispersed microstructure, and a segregation pattern occurs uniformly throughout the material, as is evident from Figure 2(a–b). These are characteristic features of spinodal decomposition. This phenomenon has also been proposed as a mechanism to explain the behavior of colloid-polymer mixtures confined between smooth planar walls[36]. Simulations showed a $t^{2/3}$ growth law of the domains with time.

The generation of these unique patterns may be attributable to a kinetic effect due to the slower diffusion of DNA molecules that accompanies drying. Therefore, the mechanism is determined by diffusion and can be treated as a diffusional problem. We can readily assume that the diffusion constant of the nanoparticles is much

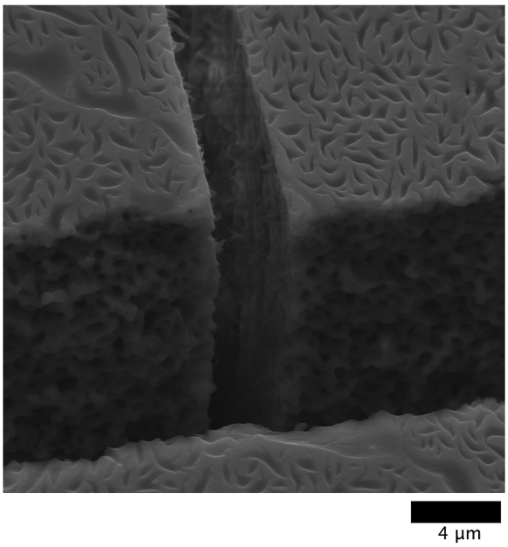


**Figure 5 | HR-SEM observation.** Intersection between a radial crack (wider) and a lateral crack (narrower) for a NP/dsDNA ratio of 1 : 0.5. The distribution of segregation domains does not seem to be affected by the cracks, which suggests that they are formed before the latter. The scale bar is 4 μm.

larger than that of the DNA molecules. The diameter of the nanoparticles is 10 nm, whereas the actual size of the DNA molecules should be in the order of one hundred nanometers based on the semiflexible character of double-stranded DNA molecules. Under the Einstein-Stokes relationship, the diffusion constant is inversely proportional to the size[37]. It is to be noted that the diameter of double-stranded DNA is ca. 2 nm, indicating that DNA molecules can get larger freedom by making parallel alignment among them while in the same time repelling nanoparticles. An increase in the net entropy due to the parallel ordering at high concentrations of rod-like molecules under repulsive interaction is the usual scenario of the formation of liquid crystals. Thus, we may expect that the net increase of the motional freedom or translational entropy is the driving force of the segregation between DNA and negatively-charged nanoparticles.

From the above consideration, we can distinguish two cases. For systems with a high nanoparticle content, we can expect a more smoothly generated segregation, since nanoparticles with a high diffusion coefficient are predominant. Usually, the characteristic length of segregation in a process of this type tends to disappear over time. This is exactly what happens with, for example, the ratio 1 : 0.125 (8 nanoparticles per DNA double-strand), for which we observe a long range order, i.e., the crescent-shape domains do not appear. For higher DNA concentrations, however, the number of DNA strands with a slow diffusion coefficient is comparable to that of the nanoparticles, and we may consider the freezing of generated micro-domains under the mechanism of spinodal decomposition. The characteristic micro-patterns are kinetically pinned due to further evaporation of the solvent, and we obtain micro-phase segregation with domains exhibiting a relatively uniform size. This is exactly what happens for the ratio 1 : 0.5 (see Figure 2), which corresponds to two nanoparticles per double-stranded DNA.

With regards to the DNA orientation, we assume that the DNA molecules tend to align in a parallel fashion during segregation, as mentioned above. This is what occurred during the segregation we observed for DNA of approximately the same size and PEG[32]. Initially, the orientation is random, but the strands tend to align in parallel due to the increasing concentration during the evaporation process. This is shown schematically on Figure 6(a). In this way, the volume occupied by the strands is reduced, and this increase in the free volume also dramatically reduces the repulsive interaction between the negatively charged nanoparticles.

We can now propose an explanation for the characteristic shape of the segregation domains. First, round-shaped domains are induced by a decrease in the water content leading to confinement. Due to the progressive parallel ordering of the confined DNA molecules, the domains cannot maintain their round shapes as the droplet shrinks. Instead, they evolve toward the crescent shape observed in Figure 2(b) for a ratio of 1 : 0.5. An explanatory illustration is shown in Figure 6(b). This represents a sound theoretical explanation that accounts for both the homogeneity and the shape of the segregation domains.

The present study is expected to contribute towards the deeper understanding of the behavior of DNA in a crowded environment. Indeed, DNA, RNA, and proteins are playing their function under highly crowded conditions within living cells[32], where negatively charged proteins are existing in large amounts. Silica nanoparticles can be seen as model compounds for such proteins (being uniform in charge and thereby simpler to describe). Another possible application is the fabrication of structured hybrid films. Such periodic self-assembled hybrid structures may serve as a useful model system for the investigation of the evaporation-driven patterning from multi-component systems[27]. In our case, the composition of the binary system before evaporation was found to be a critical factor for the formation of the periodic pattern. The homogeneously distributed crescent-shaped domains were obtained only from a specific threshold of the DNA concentration, i.e., the colloidal composition and interaction is of crucial importance. We have also here a nice example of colloidal-assisted pattern formation.

As far as extensions of the work are concerned, we will consider a more stringent control of the evaporation conditions, by systematically controlling ambient temperature and humidity. The evaporation rate and thereby the drying speed can be expected to have a crucial influence on the pattern formation observed, as the growth conditions of patterns are substantially altered. Another relevant parameter is the hydrophobicity of the substrate. As both the silica particles and the DNA strands are strongly hydrophilic, one may expect a difference in the structure of the dried pattern if the surface is significantly hydrophobic. To complement the microscopy study, one could also consider performing X-ray or neutron reflectivity measurements on the dried films. Those experiments could enable to gain information on the structure of the system on a molecular level. Finally, we are now performing theoretical studies on the dynamic segregation process with the help of computer simulations. Such studies could shed some light on the formation of the particular crescent-shaped patterns and confirm the alignment of DNA within those domains, and thereby lead to a fundamental physical understanding.

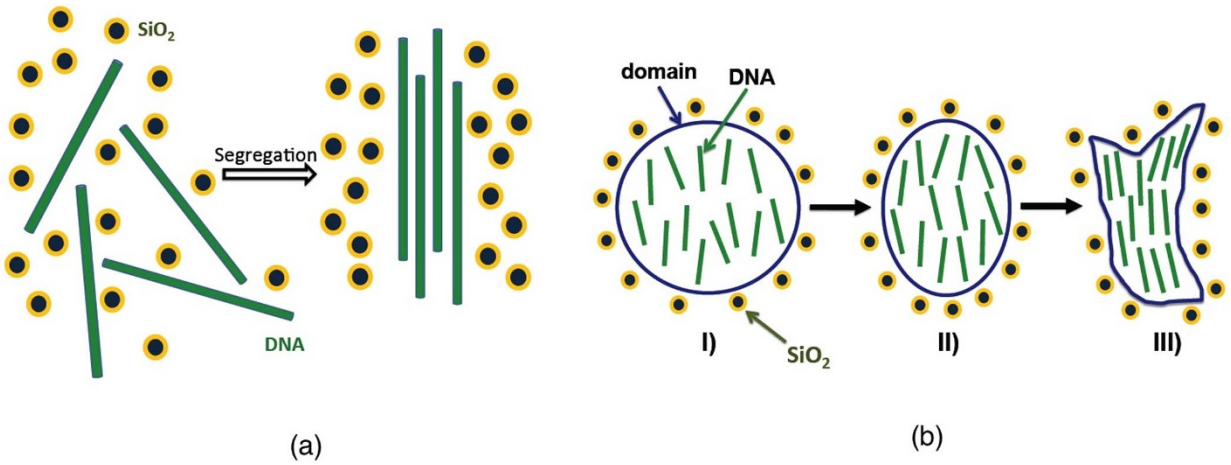


**Figure 6 | Schematic representation of the kinetic process of segregation between nanoparticles and DNA.** (a) Initially, DNA strands are randomly oriented, but tend to align in a parallel fashion as they are separated from the particles. (b): Schematic of the transition from a round-shaped segregation domain to a crescent-shaped domain. I): initial round shape with relatively disordered DNA molecules. II): intermediate state. III): final crescent shape with aligned DNA molecules.

To summarize, our results concern the expected segregation of silica nanoparticles and DNA strands, both of which are negatively charged, under confinement. This supports our previous results on the segregation of DNA molecules and alginate[28], a negatively charged polyelectrolyte, under confinement in a microsphere: i.e., under strong confinement and both species had the same charge. We have also again illustrated the effect of silica nanoparticles on the conformation of DNA strands[25,26], this time for smaller DNA strands (peak at 400 bp), which is the same size range for which we had previously reported segregation with PEG under confinement[32]. Microscopy techniques were used to characterize the patterns obtained. Especially with SEM, the patterns observed were quite remarkable, in particular for the NP/dsDNA ratio of 1 : 0.5, and fluorescence microscopy indicated that those domains are rich in DNA. We explained the formation of crescent-shaped segregation patterns in terms of kinetic and diffusional arguments in the context of spinodal decomposition. This work complements the literature on the drying of droplets that contain either DNA or nanoparticles, and is also an important contribution to the topic of segregation of DNA and negatively charged colloidal species. This phenomenon is of great importance as it could play an important role in the higher order structure of genomic DNA in a crowded cellular environment. More directly the formation of such well-defined patterned films and surfaces by simple way of evaporation induced self assembly (EISA) could be quite interesting for applications where such patterning in the range of 0.1–2 μm is demanded, such as formation of superhydrophobic surfaces, oriented or switchable surfaces, controlled wetting, etc.

## Methods

**Preparation of DNA.** For DNA, we used double-stranded DNA (dsDNA) sodium salt from salmon testes (90%, Sigma-Aldrich), with a molecular size of over 20,000 base pairs (bp). Short dsDNA strands were prepared by sonicating the large dsDNA molecules, as described previously[38]. A highly viscous solution of 5 wt% DNA in water was sonicated (Bandelin Sonorex) for 57.6 hrs in a temperature-controlled bath (5–8°C), and showed a low viscosity afterwards. To avoid a temperature that was too high, the sonication time was split into cycles of 60 min followed by a break of 15 min. This was repeated for 72 hrs to obtain the total time mentioned above. The compounds obtained exhibited a size distribution between 200 and 800 bp, with an average of around 400 bp, as shown by gel electrophoresis. The solution was freeze-dried and the DNA was stored at low temperature.

**Preparation of the drying samples.** DNA was dissolved in water to obtain a stock solution at 50 mg · $mL^{-1}$. The silica nanoparticles were commercial Ludox silica nanoparticles (30% wt. aqueous solutions, Sigma Aldrich) with a radius around 5 nm. The particles were dialyzed in Visking dialysis tubes (Medicell International) against Milli-Q water, and a 20.15% wt. stock solution was obtained. An important parameter in addition to the concentrations was the ratio between nanoparticles and DNA (double) strands. In a sample series, the nanoparticle concentration was kept constant (11.8% wt.) and the DNA concentration was varied to obtain different ratios. Control samples with either particles or DNA were also prepared. A ratio of nanoparticles/DNA double strands of 2 to 1 was obtained for a DNA concentration of 20.8 mg · $mL^{-1}$. Other ratios (1 : 0.25, 1 : 0.167, 1 : 0.125, and 1 : 0.1) were obtained by reducing the DNA concentration. A drop of solution (1–2 μL) was deposited with a micropipette on a glass or silicon wafer and left to dry under a lamp at a temperature of around 40°C. The drop did not spread over the substrate before or during drying. The drying process generally completed after 10–15 min and the thickness of the film obtained was within the range of 0.1–0.5 mm. No influence of the substrate (glass or silicon) on the macroscopic structure of the dried system was observed.

**Polarimetric microscopy.** The resulting drying patterns were observed through a JENAPOL polarization microscope (Carl Zeiss) and images were obtained at 3.2× magnification, 0.05 aperture, and 1280 × 960 resolution, with a USB microscope camera type DFK 72AUC02 with IC-Capture software (both from The Imaging Source). The polarizer and analyzer were perpendicular to each other. In some cases, movies of the drying process were also made (see ESI for ratio 1 : 0.25).

**Transmission electron microscopy.** Measurements were performed on a Tecnai $G^2$ 20 S-TWIN instrument (FEI) with a $LaB_6$ cathode operating at an acceleration tension of 200 kV. A small quantity of the sample was dropped on a copper grid, and the solvent was evaporated before measurement. The images were recorded by a CCD camera. In this case, the sample was diluted by a factor of around 100 before drying. No dilution was necessary for the other techniques.

**Scanning electron microscopy.** The samples were dried on a silicon wafer instead of a glass. They were then covered with gold powder and observed with a S-4000 high-resolution SEM instrument (Hitachi) equipped with a cold field emitter. Images were recorded by a point electronic system.

**Fluorescence microscopy.** The DNA molecules were stained with YOYO-I (Invitrogen) at a ratio of dye molecules to base pairs of 0.001%. The sample was prepared on a clean glass as described above. Fluorescence microscopy was performed using a laser scanning confocal microscope (Axiovert 100 M, Zeiss). The sample was observed with a 60× Plan Apochromat/1.4 NA oil-immersion objective lens. The excitation wavelength was 488 nm. The light was emitted from an argon gas laser and a 505 nm low pass filter was used. Under those conditions, the fluorescence emerging from YOYO-I only was detected.


1. Deegan, R. D. *et al.* Capillary flow as the cause of ring stains from dried liquid drops. *Nature* **389**, 827–829 (1997).
2. Deegan, R. D. Pattern formation in drying drops. *Phys. Rev. E* **61**, 475–485 (2000).
3. Hampton, M. A. *et al.* Influence of surface orientation on the organization of nanoparticles in drying nanofluid droplets. *J. Colloid Interface Sci.* **377**, 456–462 (2012).
4. Weon, B. M. & Je, J. H. Fingering inside the coffee ring. *Phys. Rev. E* **87**, 013003 (2013).
5. Parisse, F. & Allain, C. Drying of colloidal suspension droplets: Experimental study and profile renormalization. *Langmuir* **13**, 3598–3602 (1997).
6. Sugiyama, Y., Larsen, R. J., Kim, J. W. & Weitz, D. A. Buckling and crumpling of drying droplets of colloid-polymer suspensions. *Langmuir* **22**, 6024–6030 (2006).
7. Sen, D. *et al.* Buckling-driven morphological transformation of droplets of a mixed colloidal suspension during evaporation-induced self-assembly by spray drying. *Eur. Phys. J. E* **31**, 393–402 (2010).
8. Buck, A., Peglow, M., Naumann, M. & Tsotsas, E. Population balance model for drying of droplets containing aggregating nanoparticles. *AIChE J.* **58**, 3318–3328 (2012).
9. Isenbugel, K., Gehrke, Y. & Ritter, H. Evaporation-driven self-assembly of colloidal silica dispersion: New insights on janus particles. *Macromol. Rapid Commun.* **33**, 41–46 (2012).
10. Goehring, L., Clegg, W. J. & Routh, A. F. Plasticity and fracture in drying colloidal films. *Phys. Rev. Lett.* **110**, 024301 (2013).
11. Yunker, P. J. *et al.* Effects of particle shape on growth dynamics at edges of evaporating drops of colloidal suspensions. *Phys. Rev. Lett.* **110**, 035501 (2013).
12. Komatsu, T. S. & Sasa, S. I. Pattern selection of cracks in directionally drying fracture. *Jpn. J. Appl. Phys., Part 1* **36**, 391–395 (1997).
13. Allain, C. & Limat, L. Regular patterns of cracks formed by directional drying of a colloidal suspension. *Phys. Rev. Lett.* **74**, 2981–2984 (1995).
14. Dufresne, E. R. *et al.* Flow and fracture in drying nanoparticle suspensions. *Phys. Rev. Lett.* **91**, 224501 (2003).
15. Wang, W. N., Lin, J. Y. & Schwartz, D. C. Scanning force microscopy of DNA molecules elongated by convective fluid flow in an evaporating droplet. *Biophys. J.* **75**, 513–520 (1998).
16. Chopra, M., Li, L., Hu, H., Burns, M. A. & Larson, R. G. DNA molecular configurations in an evaporating droplet near a glass surface. *J. Rheol.* **47**, 1111–1132 (2003).
17. Morii, N., Kido, G., Suzuki, H. & Morii, H. Annular self-assembly of DNA molecular chains occurring in natural dry process of diluted solutions. *Biopolymers* **77**, 163–172 (2005).
18. Dugas, V., Broutin, J. & Souteyrand, E. Droplet evaporation study applied to DNA chip manufacturing. *Langmuir* **21**, 9130–9136 (2005).
19. Fang, X. *et al.* Drying of DNA droplets. *Langmuir* **22**, 6308–6312 (2006).
20. Fang, X. & Reneker, D. H. DNA fibers by electrospinning. *J. Macromol. Sci., Phys.* **B36**, 169–173 (1997).
21. Jing, J. *et al.* Automated high resolution optical mapping using arrayed, fluid-fixed DNA molecules. *Proc. Natl. Acad. Sci. USA* **95**, 8046–8051 (1998).
22. Abramchuk, S. S., Khokhlov, A. R., Iwataki, T., Oana, H. & Yoshikawa, K. Direct observation of DNA molecules in a convection flow of a drying droplet. *Europhys. Lett.* **55**, 294–300 (2001).
23. Smalyukh, I. I., Zribi, O. V., Butler, J. C., Lavrentovich, O. D. & Wong, G. C. L. Structure and dynamics of liquid crystalline pattern formation in drying droplets of DNA. *Phys. Rev. Lett.* **96**, 177801 (2006).
24. Maheshwari, S., Zhang, L., Zhu, Y. & C., H.-C. Coupling between precipitation and contact-line dynamics: multiring stains and stick-slip motion. *Phys. Rev. Lett.* **100**, 044503 (2008).
25. Rudiuk, S., Yoshikawa, K. & Baigl, D. Enhancement of DNA compaction by negatively charged nanoparticles. Application to reversible photocontrol of DNA higherorder structure. *Soft Matter* **7**, 5854–5860 (2011).
26. Rudiuk, S., Yoshikawa, K. & Baigl, D. Enhancement of DNA compaction by negatively charged nanoparticles: Effect of nanoparticle size and surfactant chain length. *J. Colloid Interface Sci.* **368**, 372–377 (2012).
27. Zhang, L., Maheshwari, S., Chang, H.-C. & Zhu, Y. Evaporative Self-Assembly from Complex DNA-Colloid Suspensions. *Langmuir* **24**, 3911–3917 (2008).
28. Krotova, M. K., Vasilevskaya, V. V., Makita, N., Yoshikawa, K. & Khokhlov, A. R. DNA compaction in a crowded environment with negatively charged proteins. *Phys. Rev. Lett.* **105**, 128302 (2010).

29. Yoshikawa, K., Hirota, S., Makita, N. & Yoshikawa, Y. Compaction of DNA induced by like-charge protein: Opposite salt-effect against the polymer-salt-induced condensation with neutral polymer. *J. Phys. Chem. Lett.* **1**, 1763–1766 (2010).
30. Negishi, M., Sakaue, T., Takiguchi, K. & Yoshikawa, K. Cooperation between giant DNA molecules and actin filaments in a microsphere. *Phys. Rev. E* **81**, 051921 (2010).
31. Negishi, M. *et al.* Phase behavior of crowded like-charged mixed polyelectrolytes in a cell-sized sphere. *Phys. Rev. E* **83**, 061921 (2011).
32. Biswas, N. *et al.* Phase separation in crowded micro-spheroids: DNA-PEG system. *Chem. Phys. Lett.* **539**, 157–162 (2012).
33. Gupta, S., Zhang, Q. L., Emrick, T., Balazs, A. C. & Russell, T. P. Entropy-driven segregation of nanoparticles to cracks in multilayered composite polymer structures. *Nat. Mater.* **5**, 229–233 (2006).
34. Cahn, J. W. On spinodal decomposition. *Acta Met.* **9**, 795–801 (1961).
35. Cahn, J. W. The later stages of spinodal decomposition and the beginnings of particle coarsening. *Acta Met.* **14**, 1685–1692 (1966).
36. Winkler, A., Virnau, P., Binder, K., Winkler, R. G. & Gompper, G. Hydrodynamic mechanisms of spinodal decomposition in confined colloid-polymer mixtures: A multiparticle collision dynamics study. *J. Chem. Phys.* **138**, 054901 (2013).
37. Hiemenz, P. C. & Rajagopalan, R. *Principles of Colloid and Surface Chemistry* 3rd edn, (CRC Press, 1997).
38. Prévost, S. *et al.* Colloidal structure and stability of DNA/polycations polyplexes investigated by small angle scattering. *Biomacromolecules* **12**, 4272–4282 (2011).

## Acknowledgments

We acknowledge the assistance of Christoph Fahrenson for the SEM experiments and Sören Selve for the TEM experiments at the ZELMI institute of the TU Berlin, and the assistance of Marcel Sperling (TU Berlin) for the polarization microscopy measurements. We thank Prof. Kazue Kurihara and Prof. Tadafumi Adschiri (WPI-AIMR, Tohoku University) for their support, as well as Prof. Daniel Packwood for his linguitic advice. This work was partly supported by Grants-in-Aid for Scientific Research (A) (No. 23240044, 25103012) from the Japan Society for the Promotion of Science (JSPS).

## Author contributions

The DNA was prepared by S.R. The experimental work was conducted by R.J. under the supervision of M.G. and K.Y. In addition, S.W. performed the fluorescence measurements.

## Additional information

**Supplementary information** accompanies this paper at http://www.nature.com/scientificreports

**Competing financial interests:** The authors declare no competing financial interests.

**How to cite this article:** Joksimovic, R., Watanabe, S., Riemer, S., Gradzielski, M. & Yoshikawa, K. Self-organized patterning through the dynamic segregation of DNA and silica nanoparticles. *Sci. Rep.* **4**, 3660; DOI:10.1038/srep03660 (2014).